Naval Research Laboratory

Washington, DC 20375-5000

NRL Report 9214

Signal Coherence Recovery Using Acousto-Optic Fourier Transform Architectures

K. S. WOOD, J. P. NORRIS, AND W. SMATHERS, JR.

X-Ray Astronomy Branch
Space Science Division

June 14, 1990

SECURITY CLASSIFICATION OF THIS PAGE

REPORT DOCUMENTATION PAGE

Form Approved
OMB No. 0704-0188

1a. REPORT SECURITY CLASSIFICATION	1b. RESTRICTIVE MARKINGS
2a. SECURITY CLASSIFICATION AUTHORITY	3. DISTRIBUTION / AVAILABILITY OF REPORT
2b. DECLASSIFICATION / DOWNGRADING SCHEDULE	Approved for public release; distribution unlimited.
4. PERFORMING ORGANIZATION REPORT NUMBER(S) NRL Report 9214	5. MONITORING ORGANIZATION REPORT NUMBER(S)
6a. NAME OF PERFORMING ORGANIZATION Naval Research Laboratory 6b. OFFICE SYMBOL (If applicable) Code 4120	7a. NAME OF MONITORING ORGANIZATION
6c. ADDRESS (City, State, and ZIP Code) Washington, DC 20375-5000	7b. ADDRESS (City, State, and ZIP Code)
8a. NAME OF FUNDING / SPONSORING ORGANIZATION 8b. OFFICE SYMBOL (If applicable)	9. PROCUREMENT INSTRUMENT IDENTIFICATION NUMBER
8c. ADDRESS (City, State, and ZIP Code)	10. SOURCE OF FUNDING NUMBERS PROGRAM ELEMENT NO. / PROJECT NO. / TASK NO. / WORK UNIT ACCESSION NO. DN156-066

11. TITLE (Include Security Classification)

Signal Coherence Recovery by Using Acousto-Optic Fourier Transform Architectures

12. PERSONAL AUTHOR(S)

Wood, K. S., Norris, P., and Smathers, H. W.

13a. TYPE OF REPORT	13b. TIME COVERED	14. DATE OF REPORT (Year, Month, Day)	15. PAGE COUNT
Interim	FROM 1985 TO 1989	1990 June 14	35

16. SUPPLEMENTARY NOTATION

17. COSATI CODES			18. SUBJECT TERMS (Continue on reverse if necessary and identify by block number)
FIELD	GROUP	SUB-GROUP	Acousto-optics; Fourier transforms; Data processing

19. ABSTRACT (Continue on reverse if necessary and identify by block number)

The X-ray Astronomy Branch at the Naval Research Laboratory is pursuing a program to develop a program for optical computing devices for fast processing of data in ground- and space-based applications. We have implemented a prototype one-dimensional time-integrating acousto-optic (AO) Fourier transform processor, Mark I. We have designed and built a two-dimensional hybrid (space- and time-integrating) Fourier transform processor, Mark II, that provides much higher frequency processing bandwidth, much larger dynamic range, improved signal to noise, and greatly increased speed. We describe a theory of optimum coherence recovery (CR) applicable in computation-limited environments. We have demonstrated direct acousto-optic implementation of CR in Mark I and have proven analytically that the algorithm is realizable in the Mark II system. Mark I and II have immediate astronomical relevance, e.g., for existing gravitational wave experiments, in searches for binary millisecond pulsars in the radio and X-ray bands, and in the search for extraterrestrial intelligence, as well as possible application to various signal detection problems in seismology and underwater acoustic signal reception.

20. DISTRIBUTION / AVAILABILITY OF ABSTRACT	21. ABSTRACT SECURITY CLASSIFICATION
☒ UNCLASSIFIED/UNLIMITED ☐ SAME AS RPT. ☐ DTIC USERS	
22a. NAME OF RESPONSIBLE INDIVIDUAL Kent S. Wood	22b. TELEPHONE (Include Area Code) (202) 767-2506 22c. OFFICE SYMBOL Code 4121

DD Form 1473, JUN 86 Previous editions are obsolete. SECURITY CLASSIFICATION OF THIS PAGE

CONTENTS

SIGNAL COHERENCE RECOVERY USING ACOUSTO-OPTIC FOURIER TRANSFORM ARCHITECTURES

INTRODUCTION

The program in acousto-optics (AO) conducted by the X-ray Astronomy Branch, Space Science Division, at the Naval Research Laboratory (NRL) has a special astronomical orientation—development of ultrafast analog signal processors for astronomical purposes. Time-series analysis provided the initial development challenges. This has meant that special emphasis was placed on systems that would analyze periodic and nearly periodic functions. Processers of this type also have nonastronomical applications. Our particular approach to time-series analysis is called coherence recovery (CR). It applies generally to analyses of faint, frequency-modulated functions. The frequency modulation is removed by a trial-and-error process that involves extensive computation. The faint signal becomes detectable and the characteristics of the frequency modulation are simultaneously established.

Overview

In last decade, the maturing technologies of AO components have led to declining costs, making an aggressive development program for fast processors economically feasible. A two-dimensional (2-D) Fourier processor, Mark II, for which design and procurement stages have been successfully completed, should have the equivalent throughput of two Cray-2s on algorithms such as very long Fourier transforms. The 1989 effort consisted of building Mark II and researching adaptations of the 2-D design for digital optical processing. Mark II's key assets (two Cray-2s, inexpensive to use, special features to isolate chirped signals) make it attractive for a range of applications.

Motivation

The Space Science Division AO effort is unique among astronomical groups, and the astronomical application is unique among optical computing groups. The primary thrust of the program has been to seek improvements in techniques involving Fourier transforms. The Mark II design is at the frontier of the current development. A similar processor was outlined in the literature, but it was never constructed. The current design, however, matches recently matured AO technology with real-time astronomical data processing demands. A description of one astronomical problem for which Mark II provides a solution will illuminate analogous applications in other fields.

This has meant that special emphasis was placed on systems that would analyze periodic and nearly periodic functions. Processers of this type also have nonastronomical applications. Our particular approach to time-series analysis is called coherence recovery (CR). It applies generally to analyses of faint, frequency-modulated functions. The frequency modulation is removed by a trial-and-error process that involves extensive computation. The faint signal becomes detectable and the characteristics of the frequency modulation are simultaneously established.

Manuscript approved April 8, 1989.

One of our original astronomical motivations was the search for millisecond pulsations from binary stellar systems. Such millisecond pulsars would have significant ramifications for gravitational physics. Reference 1 provides a scenario whereby a neutron star can be spun up until it becomes subject to gravitational radiation reaction instabilities. The object then becomes simultaneously a pulsar in X rays and gravitational waves. The envisioned detection strategy is to find the signal in X rays and then build a special gravity wave antenna with narrow-band response tuned to the frequency determined in the X-ray band.

Because the pulsations are expected to be weak ($<0.1\%$ modulation), long transforms are required to achieve sensitivity. In addition, the detection of such pulsations, in both electromagnetic and gravitational radiations, requires that the effect of orbital motion be removed before performing a frequency search by means of a Fourier transform (in the binary systems, which are likely millisecond pulsar candidates, the orbital parameters are partially or totally unknown but constrained). Otherwise, loss of coherence (i.e., frequency smearing) renders a weak signal unobservable. The approximate removal of orbital motion, termed coherence recovery (CR) (Fig. 1), can be effected by performing a one-parameter grid of quadratric time transformations and subsequent Fourier transforms [2,3]; one transformation of the set will provide optimal recovery over the necessary long integration time. The ideal utilization of CR is in conjunction with a very large collecting aperture. In Ref. 4 we proposed the construction of a 100-m^2 array that will detect pulsations with amplitudes $<0.01\%$ (Fig. 2).

The computational burden required for CR is determined by the large number of trial time transformations (proportional to the square of integration time) required to effect recovery. Digital implementation in real time, required for gravitational wave searches and desirable for some onboard spacecraft data processing, can be prohibitively expensive, requiring as many as 10 to 100 Cray-equivalents of computational resource. Acousto-optic Fourier processors provide direct analog techniques for fast, real-time, second-order time transformations and, hence, the best possible CR. Thus they are well-matched to various problems that involve rapid searches for frequency-smeared signals.

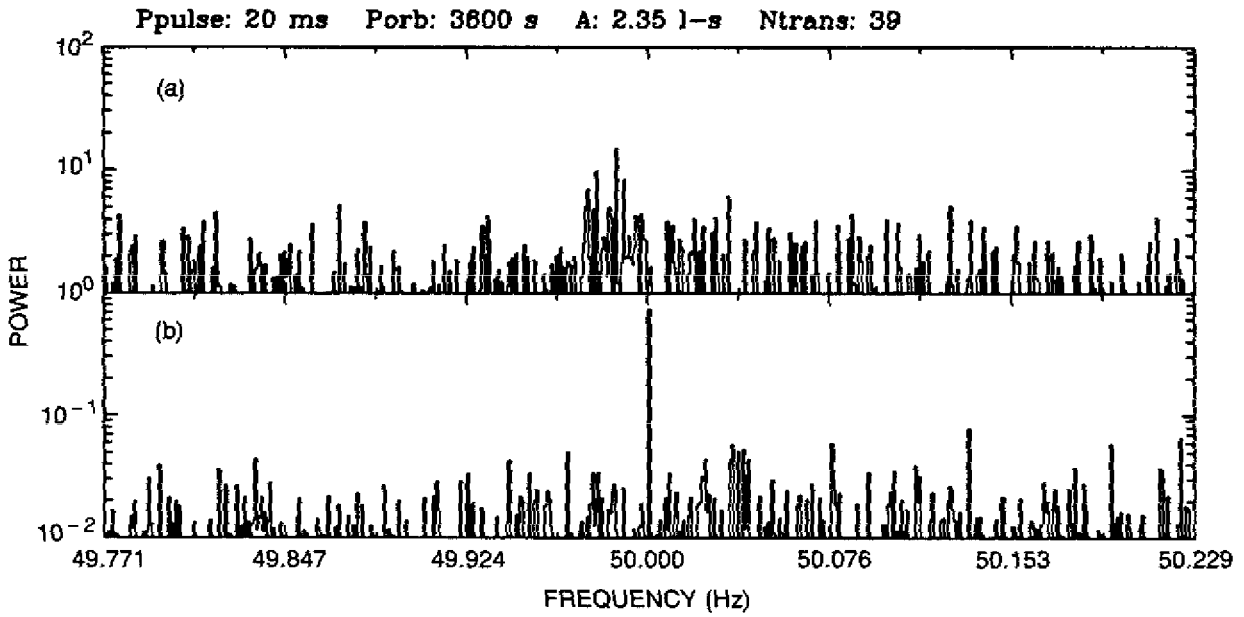

Fig. 1 — Digital simulation of coherence recovery (a) coherent signal modulated sinusoidally, plus noise and (b) optimum trial transformation recovers ~90% of original signal strength.

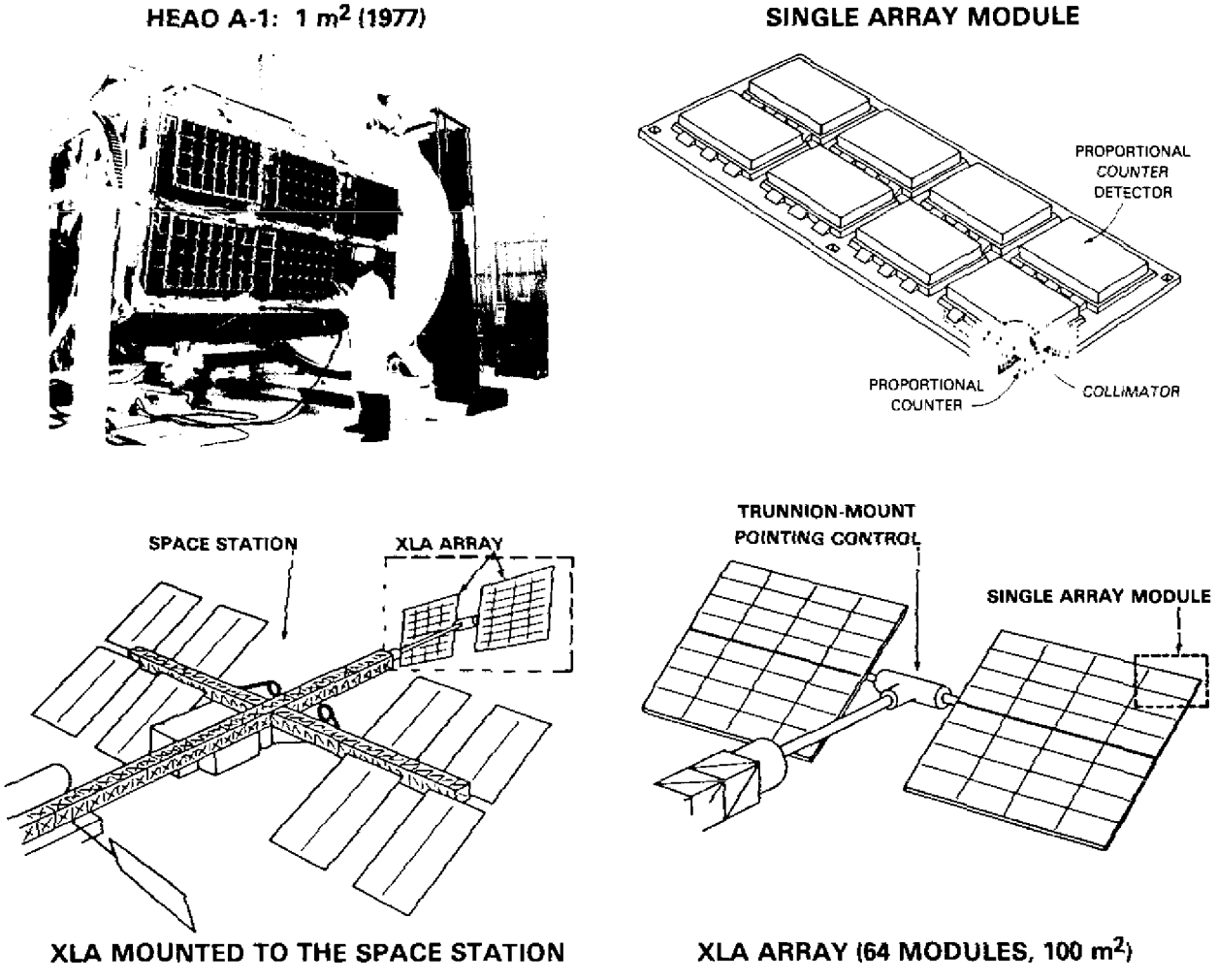

Fig. 2 — The X-ray large array

The main advantages of acousto-optics are high throughput at low cost and the promise of application in orbit to tasks such as onboard timing analysis. On board applications have the additional virtue of being resistant to soft upsets caused by charged particles. Steady improvement in ancillary technologies, such as chirp generators, is another attraction; this means that ambitious processors can now be developed at low cost.

Two-dimensional acousto-optic processors have many uses—not only on orbital platforms but also in ground-based applications. In addition to fast Fourier transforms (FFTs), acousto-optic implementations of Hilbert transforms, ambiguity functions, general correlation, and convolution are directly realized with analog techniques, thereby greatly surpassing the speed of traditional electronic devices. Development of acousto-optic processors for "speed of light" matrix manipulations using *n*-ary coding is rapidly progressing. Many astronomical data processing applications exist for these near-real-time digital optical processors. The Space Science Division's acousto-optic program, with emphasis on astronomical applications, places NRL in a unique role in both the astronomical and the optical computing communities.

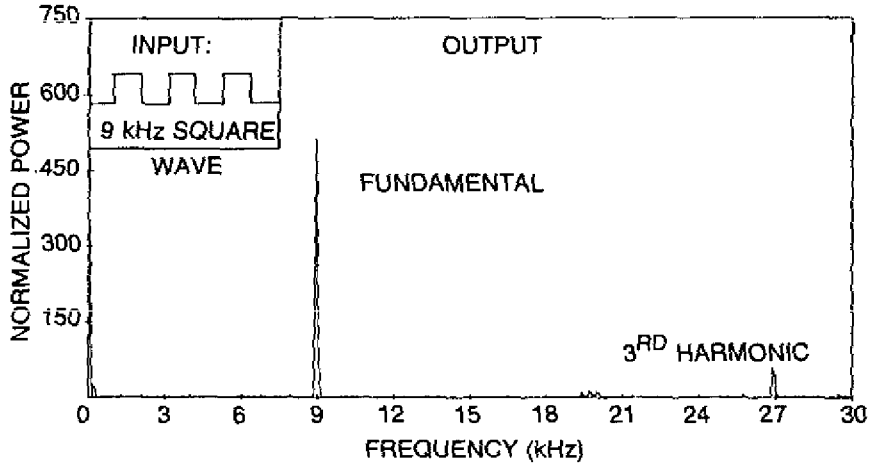

(a) 1-D Fourier processor

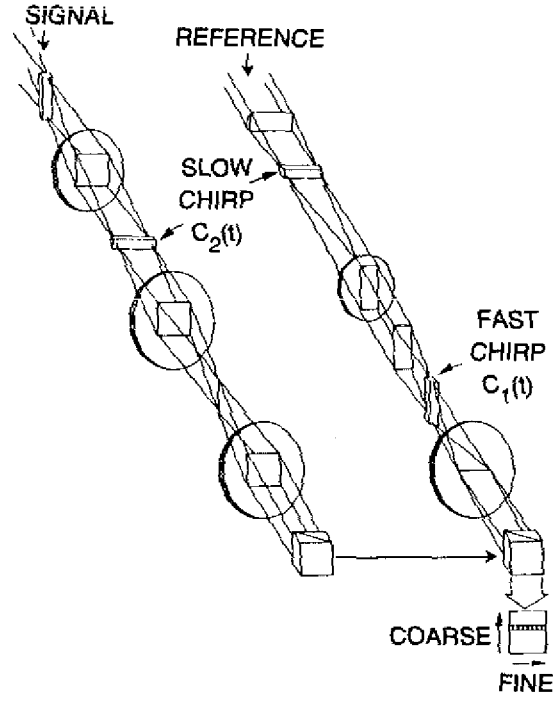

(b) 2-D Fourier processor under construction

Fig. 3 — NRL acousto-optic computer project

History and Accomplishments

The program has been active since 1986; during this time the Mark I system was constructed and tested, and Mark II was designed. This is summarized in Fig. 3. Mark I is a time-integrating architecture of modest capability (Fig. 4). It is one-dimensional, in the sense that the readout format is a 1-D display of intensity (representing Fourier power) vs position (representing frequency). After initial demonstration of system concept, Mark I was upgraded to increase its speed by a factor of 10 and to increase the number of frequency channels (Fig. 5). The scheme for CR, described briefly above, which had earlier been developed in software for pulsar-searching, was found to have a hardware realization that could be achieved with the addition of a tunable chirp. This technique is general, and it carries over to Mark II. A paper describing the CR technique and its acousto-optical implementation was presented at a meeting of the American Astronomical Society [5]. A paper on the same subject was presented at a symposium of the International Society of Optical Engineering [6].

Mark II design also occupied much of 1987. The goal is a very fast processor that can provide a 2-D output format having greatly increased bandwidth and throughput. A design was selected that can be realized in various forms, each suitable for a specific application. We began with a simple version involving only limited additional purchases and considerable recycling of Mark I components. This design was verified by using symbolic manipulator programs to check the integral transforms representing the nominal performance. A key component of Mark II, the fast chirp driver that implements coarse separation of frequencies, represents an important improvement in 2-D Fourier processors.

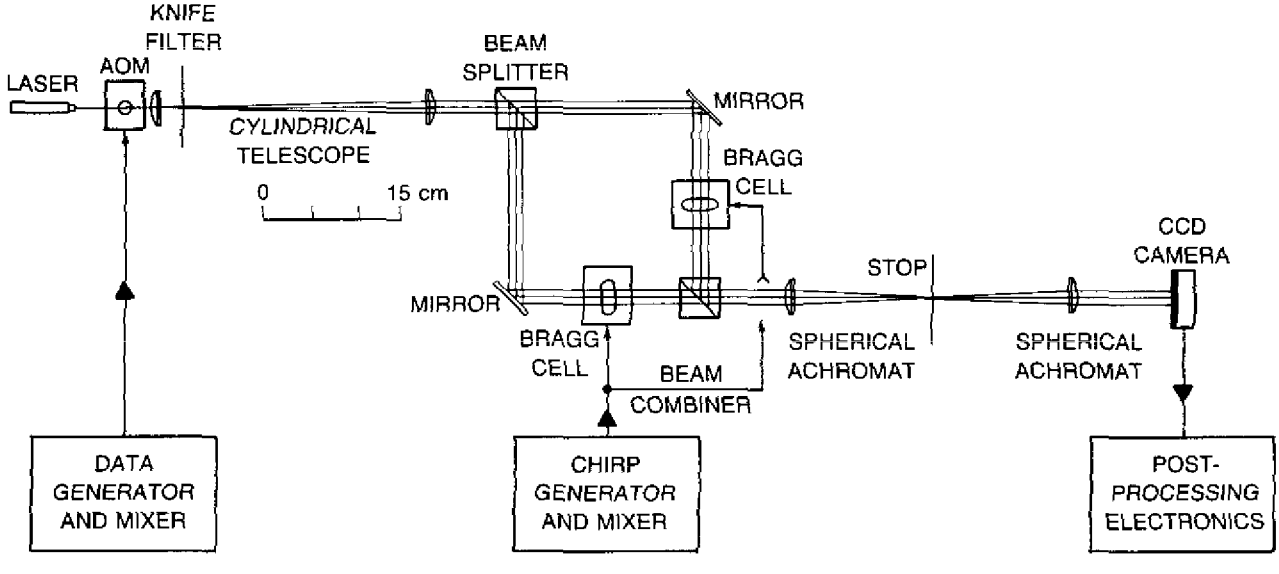

Fig. 4 — One-dimensional time-integrating Fourier transform architecture

MARK I ARCHITECTURE: ONE-DIM
T-I FOURIER TRANSFORM PROCESSOR
BUILT APR - MAY '88

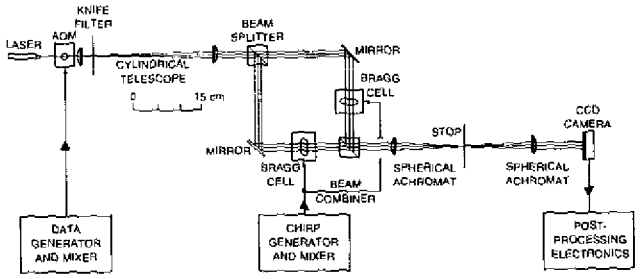

FIRST FOURIER TRANSFORMS PRODUCED BY
MARK I. 4 KHZ AND 8 KHZ SIGNALS.
NO OPTIMIZATION. JULY '86

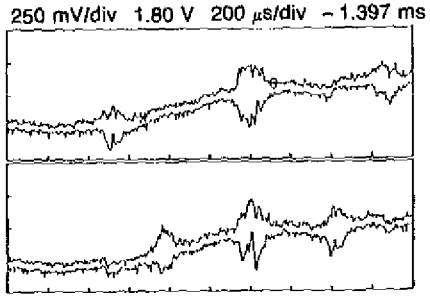

OPTIMIZATION IMPROVES RESOLUTION,
SPEED, DYNAMIC RANGE. 10 KHZ AND
15 KHZ SIGNALS. SEP - OCT '86.

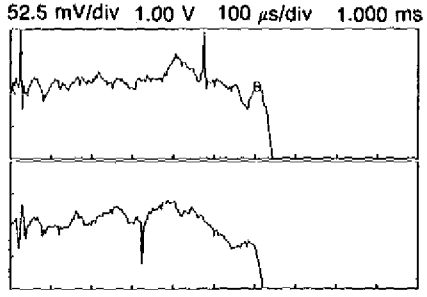

LINK TO IBM AT COMPUTER ENABLES
DIFFERENCING, SIGNAL - BACKGRD.
AMPLITUDE SPECTRUM. NOV '86.

POWER SPECTRUM OF PREVIOUS FIGURE.
ACHIEVE ULTIMATE RESOLUTION, < 2
PIXELS/FREQUENCY CHAN. NOV '86.

FOURIER P. S. DECOMPOSES SQUARE
WAVE; POWER IN FUNDAMENTAL AND
3RD HARMONIC IN CORRECT RATIO.

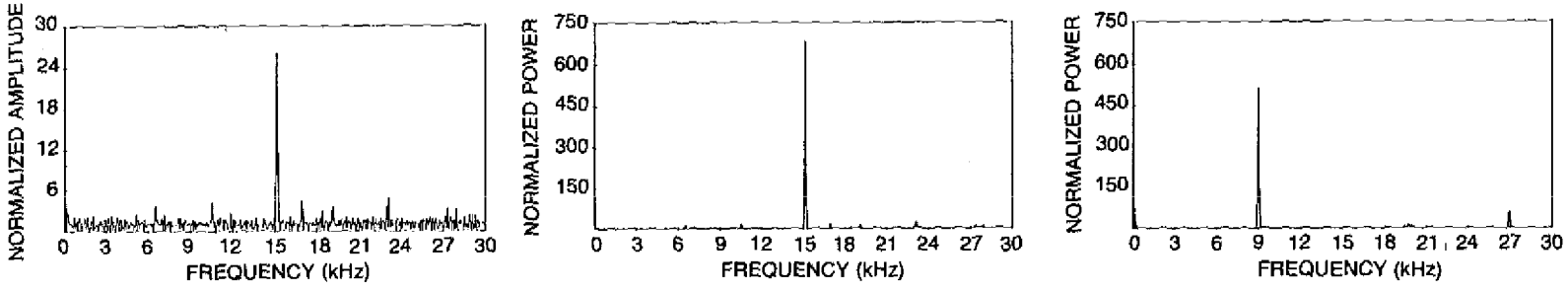

ACOUSTO-OPTIC FOURIER TRANSFORM PROCESSORS

Fig. 5 — Refinements and upgrades in Mark I yield improved spectral results

MARK I: ONE-DIMENSIONAL TIME-INTEGRATING FOURIER PROCESSOR

Design and Concept

The design of Mark I resurrects a proven architecture for exploratory purposes. The original version of this time-integrating Fourier architecture was first proposed and implemented by the Optical Sciences Division at NRL [7]. The use of a similar architecture provided a working model to implement major modifications (CR) and advance to a design for a 2-D Fourier system.

Figure 4 shows the geometry of the Mark I processor; this may facilitate comprehension of the operating principles involved. Mark I is composed of a front end, where data are applied to an AO modulator to modulate a laser; a cylindrical telescope operated in reverse that produces a horizontal sheet beam; a central interferometer segment that creates a Fourier kernel; and a time-integrating output arm in which the kernel beats with the (temporal domain) input to compute the (frequency domain) output. The kernel is actually realized upon recombination of the two beams at the detector camera plane, where most extraneous phase terms cancel identically. Here, the spatial coordinate of a 1-D sensor is related to the Fourier frequency coordinate. Stops designed to remove the (unwanted) undiffracted parts of the beam also appear. Reference 8 provides a comprehensive treatment of many aspects of AO signal processing.

In AO Fourier architectures, the signal may be introduced by intensity or frequency modulation of the light beam; for the design shown in Fig. 4, the method is intensity modulation. The signal is subsequently carried in both legs of the interferometer. Here two counterpropagating, chirped sinusoids (of form $\exp\{i\alpha t^2\}$, α = constant) are impressed onto the light beams by frequency modulation using Bragg cells (acousto-optic beam deflectors, AOBDs). The momentum-matching conditions between the light and sound waves within the AOBD require either increasing or decreasing the light frequency by the sound frequency; this is sometimes referred to as up and down (frequency) shifting of the light. Selection of either the first plus or minus diffraction order determines whether the light is up- or down-shifted, respectively. The Fourier kernel results from heterodyning the up- and down-shifted beams. The relative light frequency lag between the two sheet beams (a function of AO cell spatial coordinate, and therefore of detector coordinate) provides a difference frequency—the Fourier kernel.

It may help to think of this arrangement as a bank of frequency filters. One such filter tests for the presence of a periodic component at one discrete frequency, at one spatial location in the detector plane, by maintaining a (temporal) sinusoid that is heterodyned with any arbitrary input. The bank of filters maintains a series of such sine waves, one at every frequency within a certain bandwidth, and the frequency so maintained advances uniformly as a function of spatial position within the device. At the output camera, the detected signal builds up continuously in one channel over the course of an integration cycle. These are the essential features of a time-integrating Fourier architecture. In addition, heterodyning of the input with all the filters whose frequencies differ from the input signal frequency produces a light bias that builds up in all channels; the signal is detected against this background.

By contrast, a space-integrating Fourier architecture simply uses one Bragg cell to diffract an input beam at angles that are proportional to the frequencies present in the signal. The diffracted beam is then passed through a spherical lens that accomplishes the Fourier transform. The light bias built up over an integration period is insignificant compared to that in a time-integrating processor and

is essentially attributable to stray laser light. Hence, the detected light represents only the signal; this is an important feature of space-integration. However, space-integration does not allow for extended temporal integration. Also, in the context of AO Fourier processing, a 2-D, purely space-integrating architecture cannot be implemented. The distinctions between time-integrating and space-integrating architectures must be kept in mind for the discussion of Mark II, because both time- and space-integrating geometry are combined to generate the 2-D folded Fourier output of that architecture, while the beneficial aspects of the two approaches are retained.

Optical Bench and Associated Electronics

The project moved very quickly from inception to development of Mark I. This was partly because components were initially borrowed from another NRL code. Availability of those components dictated details of the first-generation Mark I layout, but upgrades were later made to improve performance.

Upgrades in AO equipment during the Mark I phase were made to increase the data-processing speed of the system. A new AO modulator was purchased that introduced data by intensity modulation at rates as high as 10 MHz. To Fourier analyze data introduced at these higher rates, a faster chirp generator was obtained. This chirper is a linear voltage-controlled oscillator (VCO) that we were able to operate at a 1-ms chirp rate (the effective integration period). Faster usable chirp rates, which would take advantage of the ultimate speed of the AO modulator, are obtainable from the VCO chirper by introducing more sophisticated synchronizing electronics. More important from the standpoint of new algorithms, by using both our analog chirper and a digital chirp synthesizer, we were able to demonstrate CR in the AO system (described below).

An IBM PC was set up to direct control of the AO processor's input and output. Computer programs were devised that communicated with a digitizing oscilloscope, a chirp synthesizer, and a data generator; they also processed the signal received from the AO system. At the later stages, the computer provided test signal inputs for the data generator. These inputs were tailored to simulate frequency-smeared signals on which the AO system performed simultaneous CR and Fourier analysis. The next two sections describe the progress made with component upgrades and the invention of an AO system capable of CR.

Performance

Mark I underwent a series of improvements from July 1986 to January 1987, reflecting our learning curve and increasing skills in applying the basic principles of optical techniques. The first test of Mark I was very crude; initially it was possible to resolve an 8 kHz input band into a few frequency channels. Various optimizations improved the figures of merit until the appearance of the analog signal was a sharp spike. Following this, much further improvement was realized by utilizing the postprocessing capability of the PC for such tasks as digitizing output signal waveforms, computing signal minus background, and finally presenting power spectra. By December 1986, it was possible to exhibit a square wave input analyzed into the first and third harmonics in the proper ratio. Design iterations, which incorporated faster analog input electronics, led to system performance closer to the intrinsic limits of the AO components. During this period the resolution increased from <50 channels to ~ 400 channels while the input rate increased from 15 to 350 kHz. Progress in the development of Mark I is illustrated by the quality of spectra obtained (Fig. 5).

Coherence Recovery

A by-product of the Mark I effort was the discovery of an AO method for handling sinusoids chirped by arbitrary functions. It was motivated by the original astronomical application—to detect faint, fast pulsars in binary systems. The problem is that the binary motion of the source alternately blue shifts and red shifts the signal, i. e., the signal is frequency modulated (smeared in frequency space). The simplest way to undo this process would be to compensate the data by using the binary orbit parameters, which is the standard technique in pulsar work. Unfortunately, the orbit is unknown in nearly all cases. A full search of the space spanned by the amplitude, frequency, and phase of the unknown orbit is computationally prohibitive with present resources. However, searches of a one-parameter grid of parabolae (quadratic transformations) have been used to achieve comparatively high sensitivity by using the SSD VAX [2]. The set of parabolae can be thought of as a grid of approximations to the actual, unknown orbit. (The VAX takes $\sim 1/4$ h to do a 2^{20}-point Fourier transform. An optimized Connection Machine FFT will take ~ 2 s for 2^{20} points [9]. This is part of the overall program motivation—AO processors would be much faster.) This algorithm may be used to achieve approximate CR over an interval that is short compared to the orbital period. Our simulations (Fig. 1) show that $>90\%$ of the power actually present in the coherent signal can be recovered.

We have discovered an analog AO technique for CR that is identical to a quadratic transformation. The technique was implemented with minor additional hardware development [6]. We found that CR can be achieved in Mark I by making the two chirps slightly unequal. Varying the difference in chirp accelerations over a small range generates the required set of quadratic transformations. The resulting modification to the Fourier kernel includes an additional fringe term (with entirely negligible effect in practical applications) and a quadratic phase term that accomplishes the exact function of the grid of parabolae as in the software implementation. Although many conceivable applications involve sinusoidal (or arbitrary functional) modulation over a fraction of a cycle, for which approximate CR is obtainable, linear frequency excursions (red or blue, growing linearly with time) can be $\sim 100\%$ recovered with this algorithm. Linear frequency excursions $>25\%$ have been successfully recovered in Mark I. The fact that the technique is analog (no complex digital premodification of chirp accelerations is necessary) makes it fast and very attractive. Certain specific applications might more profitably search a different family of functions to effect a good coherence recovery. In this case, preparation of chirps might be implemented with dedicated digital hardware, rather than with software. The quadratic transformation often will be the best one-parameter approximation. Appendix A develops mathematics for CR for the case of pulsars in binary orbits, together with AO realization of this case.

Astronomical applications of the CR algorithm include real-time searches for radio and X-ray pulsars, searches for continuous-wave gravitational radiation from the most rapidly spinning pulsars, and SETI (search for extraterrestrial intelligence). In addition to the astronomical uses, potential applications of the CR algorithm implemented with AO processors exist in other fields, i.e., in problems where the sensitivity for real-time detection of chirped signals may be increased by compensating the effect of modulation by an arbitrary function. The algorithm is applicable to situations where, during the observation interval, the phase (frequency) modulation is sufficiently close to quadratic (linear) in time, or where the observation interval is limited so that this condition obtains. Such devices may be adapted to problems involving propagation of waves in inhomogeneous media, e. g., in such disciplines as seismology and underwater acoustic signal reception.

With the emergence of the CR concept, Mark I development was regarded as mature. A paper was published describing the general CR concept and its realization in a 1-D time-integrating design

[6]. At this point in the program, limitations were being approached because of the 1-D nature of the Mark I device. It would be possible to improve upon the Mark I and make small packages suitable for various purposes. However, in such systems integration time (and therefore sensitivity) is limited. Also, the 1-D format affords intrinsically low resolution and therefore comparatively poor performance when measured against a computer such as a Cray. The major purpose of the program was to build simple systems that could compete with Crays on algorithms such as Fourier transforms.

MARK II: HYBRID (SPACE AND TIME INTEGRATING) TWO-DIMENSIONAL FOURIER PROCESSOR

Mark II is a 2-D hybrid architecture with performance figures of merit that, in some respects, exceed those of a Cray-2. The 2-D output format resembles a raster scan of frequency space. Hybrid refers to the combination of space-integrating and time-integrating subsystems that are used to achieve an effective one-parameter (frequency) readout format. The entire Fourier transform is realized in piece, on repeated passes of the input, more rapidly than a Cray can accomplish the same computation. The throughputs (bits/second processed and recorded) are comparable. The AO processor's bit accuracy is less than that of the digital computation, so that the principal gain is in speed. In fact, Mark II computes a 10^6-point Fourier transform approximately 500 times faster than does a Cray-2.

A significant compromise has been accepted in the area of greatest advantage, namely speed. This compromise is the repeated introduction of the input, made necessary by the choice of a comparatively limited camera for output-recording, one with an $\sim 256^2$ pixel format. The repeated passage of the data through the system is required by the need to move the small camera around in the output plane so that it records the full "image," i.e., the Fourier transform, as a mosaic of smaller images. (In practice, subsets of the output bandpass are electronically selected and appear within the camera's stationary format.) This compromise has been accepted because the goal is to demonstrate the principle of a hybrid architecture in the most expeditious manner. Although performance of the prototype will be suboptimal, its overall speed can, in principle, be easily upgraded by using a readout camera that captures the entire Fourier spectrum in one frame.

The architecture described below is realizable in a variety of distinct configurations, each of which serves a different purpose. The general idea of a 2-D frequency format has existed for some time. Mark II is a modification of a design that was initially described in Refs. 10 and 11 but never constructed. The reason for the delay between conception and attempt at implementation is, essentially, that two key hardware components that were required for the originally intended application did not exist. These components were an output camera having a readout speed faster than any that exist even today (by several orders of magnitude) and a chirp device capable of excursions of a few hundred MHz/few ms. Thus there was a poor match between available technology and the intended purpose. In contrast, for the intended astronomical applications, Mark II is a high-performance device that is available with current technology. Moreover, the fast chirp device used an innovative design. Having incurred the primary setup cost in developing Mark I, the further cost for Mark II has been minimal. We now turn to a more detailed description of the various points just introduced.

Expected Performance

The expected performance of Mark II derives straightforwardly from the parameters of key components. Appendix B provides the predicted figures of merit, comparisons with the Cray-2, and

specifications. The camera specification (62500 pixels) (Table B1) shows that we should approach a bandwidth of 2^{15} frequency channels. We assume that, as in Mark I, the limit of pixels/2 will be attained. Two new tellurium dioxide AOBDs increase the center operating frequency to 350 MHz (with a 3 dB bandwidth of 200 MHz); this determines the maximum signal input frequency and, therefore, the data rate. The dynamic range is expected to be ~ 500, which is a substantial factor of 20 increase over systems that are of a fully time-integrating rather than hybrid design. This results from a combination of the low light bias associated with the space-integrating dimension and the use of the single-sideband method of introducing the input signal. Thus Mark II has the capability of finding weak signals in the presence of strong, saturating signals. The space-integrating feature also provides a gain in bandwidth of about a factor of four over purely time-integrating systems. The throughput (Table B2), which results from considering input rate, bit accuracy, and the number of times the input must be recycled to accommodate the output camera, is about double that of a Cray processing the same transform.

Design and Concept

Like Mark I, the architecture of Mark II is composed of two separate legs of an interferometer; each leg produces a resultant signal at the output camera (Fig. 6). In a wideband, fast processor like Mark II, coherent Fourier integration over a long input data stream is desired. The wide bandwidth is accomplished by using two kinds of chirps. In Mark II, the two light beams carry a coarse chirp (reference leg) and the input data (signal leg), both introduced by using the 350 MHz AOBDs. The coarse chirp leg uses a fast repeating VCO, which is the most demanding chirp generator in the system. The device must sweep 100 MHz ± 1 Hz (we plan to use only half the bandwidth of the new AOBDs) each 3 μs and return to the same starting phase ($\pm 1°$) each repetition. Without return to fiducial phase and frequency at the start of each chirp, the integration would not be coherent. The wideband AOBDs, together with the spherical lenses that follow them constitute the space-integrating portion of the system. The narrow-band, slow chirps are introduced into both legs, propagating in AOBDs aligned perpendicular to the space-integrating AOBDs. The geometry and operation of the horizontal (slow chirp) dimension is similar to that in the Mark I processor. The integration is carried out over the duration of the slow chirps. The interference of all signals produces a 2-D format Fourier kernel at the output camera, which is a focal plane of the system. The effective mathematical kernel, however, is 1-D: the processor performs a continuous, coherent integration over only one variable—time (Fig. 7). The space-integrating arm produces the coarse-frequency vertical dependence in the output, which appears as a succession of lines. These lines are associated with a repeating delta function of the vertical coordinate, which arises from recycling the fast chirp. The horizontal direction is the fine-frequency direction and is produced by the slow chirp entered into both arms. A sinusoidal input will produce a single bright line (the line containing the input frequency); along this line will be a single bright point at the coordinate, which represents a fine measure of the input signal frequency.

Thus four AOBDs are in the design—two accept the slow, fine chirp; one accepts the fast, coarse chirp; and one accepts the data stream. These signals are folded together by lenses in the system; the result can be represented as a convolution integral [10, 11]. When the integral is evaluated to calculate expected performance at the output plane, the result is an expression having parts that stand in one-to-one correspondence with the salient features of the output format. Appendix C presents a complete mathematical representation of the waveform interactions in Mark II from input to output. The mathematical treatment was verified by using the Symbolic Manipulation Program, as described of the end of this section.

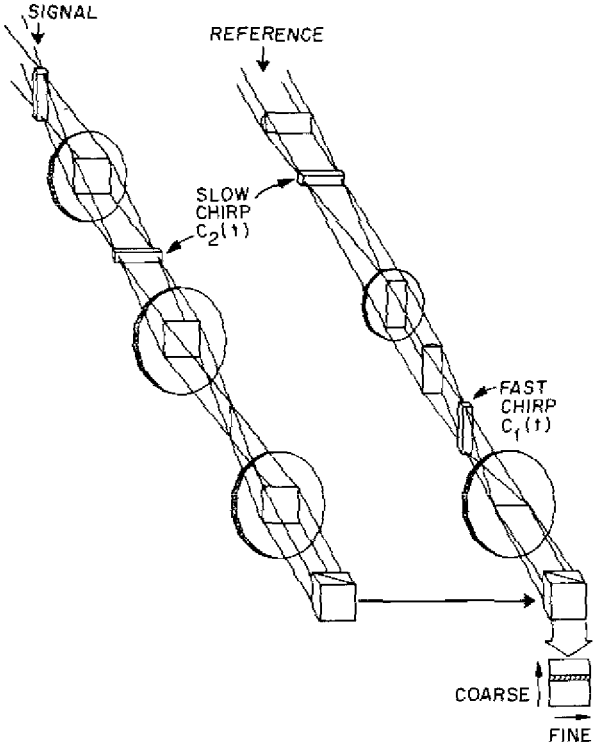

Fig. 6 — Mark II: Two-dimensional format, hybrid (space-and-time-integrating) architecture. Folded one-dimensional Fourier transform processor, a signal searcher with AO capability for recovery of smeared signals.

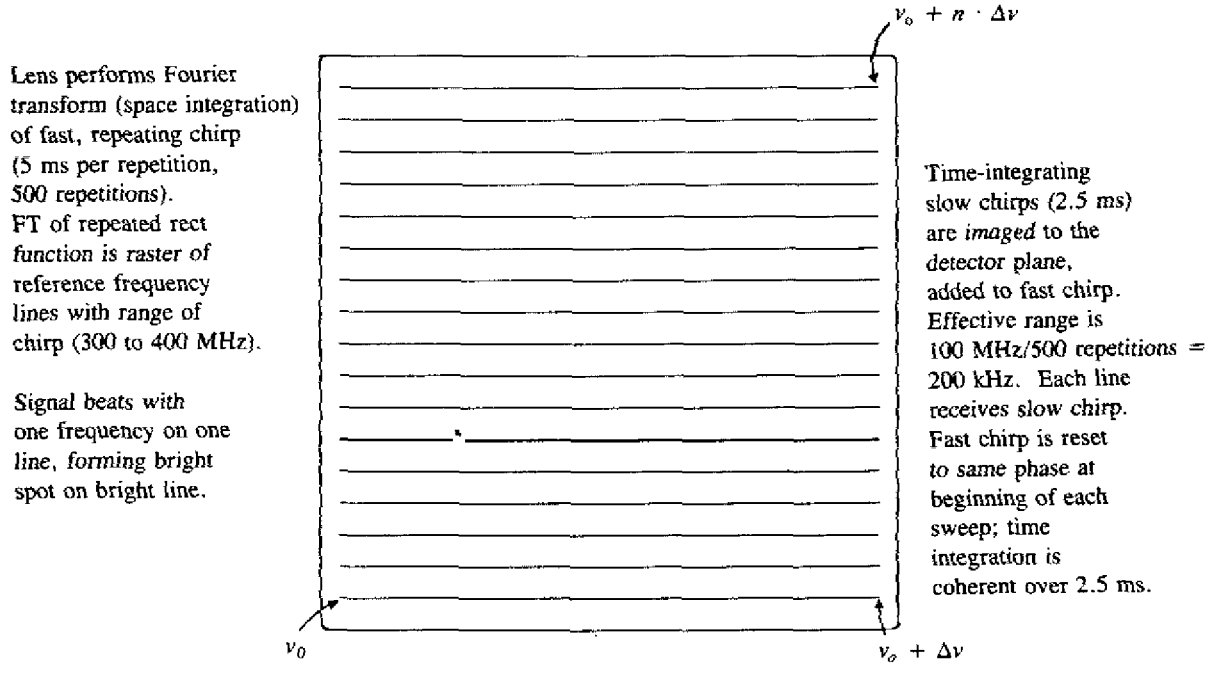

Fig. 7 — How Mark II performs 1-D Fourier transform in 2-D
(2-D format is effectively a folded 1-D Fourier transform)

Coherence Recovery in Two Dimensions

As in Mark I, implementing the CR technique in Mark II requires mixing two slow unequal chirps [6]. The 2-D format does not affect the validity of the method. A frequency-smeared signal that would otherwise have overlapped two coarse frequency lines is recovered at one point on one line for the optimum quadratic transformation. Moreover, since the Mark II output is formatted in two independent spatial dimensions, the processor can be designed for either of two general classes of problems:

- applications similar to the astronomical CR problems described in Section 1 where the 2-D format is effectively a long 1-D frequency format with high resolution and the quadratic transformations are applied consecutively; or
- applications (perhaps not astronomical) in which rapid CR is desired and low-frequency resolution will suffice, where one dimension is the frequency coordinate and the other simultaneously accommodates parallel processing of all the quadratic transformations.

The next two sections describe architectures of these types.

High-Resolution, Large Bandwidth Serial Architecture

In the high-resolution Mark II processor, the CR concept can be realized in several forms that differ in how the slow chirps are introduced. The slow chirps may be applied in at least two additional geometrical configurations besides the "additive" architecture shown in Fig. 6 (see Ref. 12 for a discussion of additive and multiplicative architectures). First, both slow chirps may be introduced by using AOBDs in a single arm of the architecture, with accompanying lenses rearranged for the required imaging and spatial Fourier transformations. The effective difference in acceleration, which is incurred by the angular compression (from frequency-dependent Bragg diffraction) of the first chirp when traveling the distance to the second Bragg cell, can be compensated by a base difference in acceleration between the two chirps. Difference in acceleration greater than this frequency offset provides CR. This "multiplicative" arrangement is apparently not described in the literature. An alternative multiplicative design uses one slow chirp applied through an AO spot modulator, in the arm that contains the slow chirp AOBD, or in the opposing arm [10,11]. In any one of these three configurations, the difference in acceleration between the two slow chirps, which constitutes the CR portion of the chirp, may be created separately as a third chirp and single-sidebanded with the signal or with the coarse chirp, instead of appearing in one of the slow chirps. The latter alternatives for CR emphasize a more symmetrical design (with both slow chirps having equivalent acceleration), but they do not provide a materially different result. Relative advantages of each arrangement derive primarily from convenience in hardware combinations since the mathematical descriptions are similar.

In all of the foregoing arrangements, the several quadratic transformations required to achieve CR are performed serially. Thus, for 10^3 transformations, at 3 ms per run, the entire set of transformations is evaluated in ~ 3 s. The merit of this kind of processor is high frequency resolution across a large bandwidth.

Ultrafast Parallel CR Architectures

Mark II can be modified to perform $\sim 10^3$ time transformations in parallel with a reduced number ($\sim 10^3$) of frequency resolution elements. This modification would provide the capability of detecting weak signals from sources undergoing rapid acceleration or from signals that pass through

SMP calculation that simulates Mark II performance, symbolically calculating the output as a function of the input. Results of selected stages are shown and annotated to indicate their relationship to components of the processor.

FUTURE DEVELOPMENTS

The program orientation remains development of processors for astronomical data, either on the ground or in orbit. At some future point it may become important to explore packaging of such processors for space flight.

An ambitious extension of Mark II is contemplated that could provide precision equal to that of a digital machine. We are considering developing a digital acousto-optical array processor in which some aspects of the design resemble a generalized Mark II architecture. This array processor would be capable of linear operations with throughputs (approaching 10^{12} bits/s) almost two orders of magnitude greater than those of state-of-the-art digital supercomputers; it would overcome the limitation of inadequate precision that is inherent in many analog processor systems.

ACKNOWLEDGMENTS

The authors express their gratitude to several individuals who greatly influenced this work. Dr. Herbert Gursky initially suggested investigation of acousto-optic computation. Drs. John Lee and Ravi Athale provided guidance in selecting among approaches to the task. Dr. Bruce Wald facilitated establishment of our collaborative arrangement with NRL Code 8133. Dr. W. Collins and Dr. C. Gilbreath generously provided not only hardware components but also took an interest in the program and provided many consultations on architectures and technical approaches. Dr. T. Bader originally conceived and suggested to us the baseline design of the Mark II architecture. This work was supported by the Office of Naval Research.

REFERENCES

1. R.V. Wagoner, "Gravitational Radiation From Accreting Neutron Stars," *Ap. J.* **278**, 345 *(1984).*

2. J.P. Norris and K.S. Wood, "Discovery of 5 Hertz Quasi-Periodic Oscillations in Cygnus X-2," *Ap. J.* **312**, 732 (1987).

3. K.S. Wood, J. Norris, P. Hertz, and P. Michelson, "Millisecond X-ray Binary Pulsars" *Proc. Conf. on X-ray Variability of Compact Objects*, A. Treves, ed. (Milan: Associazione per l'Avanzamento del' Astronomia, 1986.

4. K.S. Wood, et al. Concept Study of the X-Ray Large Array [XLA] for the NASA Space Station" (1985).

5. J.P. Norris, K.S. Wood, and H.W. Smathers, "Acousto-optic Fourier Transform Processors for Astromical Applications," *Bull. A.A.S.* **19**, 748 (1987).

6. J.P. Norris, K.S. Wood, and H.W. Smathers "Signal Coherence Recovery Algorithm for Acousto-Optic Fourier Transform Architictures with High Bandwidth," *Proc. SPIE.* **936**, 213 (1988).

7. J.N. Lee, S.-C. Lin and A.B. Tvetan, "Discrete Fourier Transformation Using a Time-integrating, Acousto-optical Signal Processor," *Appl. Phys. Lett.* **41**, 131 (1982).

8. N.J. Berg and J.N. Lee (ed.), *Acousto-Optic Signal Processing* (Marcel Dekker, New York 1983).

9. J.P. Norris, P. Hertz, K.S. Wood, and P. Anderson, "Algorithms for Long Fast Fourier Transforms on a Connection Machine," in *Proc. 2nd Symposium on the Frontiers of Massively Parallel Computation* (1988).

10. T. Bader, "Coherent Optical Hybrid Techniques for Spectrum Analysis," *Proc. SPIE* **185**, 140 (1979).

11. T. Bader, "Acousto-Optic Spectrum Analysis: A High Performance Hybrid Technique," *Appl. Opt.* **18**, 1668 (1979).

12. I.J. Abramovitz, N.J. Berg, and M.W. Casseday, in *Acousto-Optic Signal Processing*, Berg and J. Lee, eds. (Marcel Dekker, New York, 1983), pp. 291-297.

Appendix A

COHERENCE RECOVERY OF A FREQUENCY-MODULATED SIGNAL BY USING QUADRATIC TIME TRANSFORMATIONS

For an emitting source undergoing arbitrary acceleration, a grid of transformations must be applied in a space of arbitrary dimension to achieve optimal CR in only one transformation of the set. For many applications, a quadratic approximation over a short portion of the trajectory of points in n-parameter space may be sufficient to detect an otherwise unobservable signal. The great value of this method is that the quadratic approximation requires only one parameter, thereby resulting in a substantial saving of computation time and resources. In most cases of astrophysical interest, the signal arises from a source in a binary orbit, which is an ellipse. A circular approximation to an elliptical orbit provides an adequate example of the contraction of parameter space from three variables to one and does not detract from the validity of the treatment.

Coherence Recovery in Binary Stellar Orbits

For a circular orbit the observed signal is advanced or retarded by a time of maximum amplitude A, the projected radius of the orbit expressed in light seconds, with respect to the center-of-mass frame. The system revolves with frequency $\Omega = 2\pi/P_{\text{orb}}$, where P_{orb} is the orbital period. The phase lead/lag may be expanded in a Taylor series to second order (an arbitrary orbital phase ϕ_0 is neglected for simplicity):

$$\delta\phi = A \cdot \sin(\Omega t)/P_{orb} = A[\sin(\Omega T_o) + \Omega\cos(\Omega T_o)t - \Omega^2 \sin(\Omega T_o)t^2/2]/P_{\text{orb}}. \qquad \text{(A1)}$$

T_o, the time about which the function is expanded, can be taken to be the center of observation. The first term of the expansion represents this fixed point in phase with respect to the orbit; it is of interest only in absolute phase studies. The second term represents an average Doppler shift for the interval of observation and contains no broadening effect since it is linear in time; pulses arriving P_{pulse} seconds apart will be compressed or expanded by $\pm[1 + \Omega A \cdot \cos(\Omega T_o)]$, which is a constant factor. The last term constitutes the lowest order smearing or broadening effect in phase of arrival and, therefore, in frequency. This term is quadratic in phase and linear in frequency, and it attains a maximum when the argument of sin is $\pi/2$. Hence when the source exhibits zero Doppler shift (second term), the broadening is greatest and can be of positive or negative "curvature." A quadratic approximation applied to the time of arrival of the sampled events will compensate for the phase lead or lag:

$$t' = t + \Omega^2 A \cdot \sin(\Omega T_o)t^2/2 = t + \alpha t^2 . \qquad \text{(A2)}$$

The number of transformations required to cover positive or negative curvatures for observations of worst case ($\Omega T_o = \pi/2$) is

$$N_{\text{tran}} = \alpha_{\max}/\delta\alpha = (A\Omega^2/2)/(P_{\text{crit}}/2T^2). \tag{A3}$$

The expression for δ_α, derived below, assumes a program that searches for optimal recovery, which is desirable when the signal may be barely detectable. Equation (A3) can be rewritten as

$$N_{\text{tran}} = A(2\pi T/P_{\text{orb}})^2/P_{\text{pulse}} \tag{A4}$$

if P_{pulse} is near $P_{\text{crit}} = P_{\text{Nyq}}$. Otherwise, the required number of transformations is reduced by a factor $P_{\text{pulse}}/P_{\text{Nyq}}$. In a search problem, P_{pulse} is not known a priori, and therefore the maximum number of transformations is required. Note that N_{tran} is proportional to $(2\pi T/P_{\text{orb}})^2$. Moreover, $2\pi T/P_{\text{orb}}$ must be small for the approximation to be valid. As $2\pi T/P_{orb}$ grows, the higher order terms become more significant, and quadratic CR becomes less optimal. The third-order term is important when, assuming a phase $\Omega T_o = \pi/4$,

$$A\Omega^3 T^3/6 \sim A\Omega^2 T^2/2,$$

therefore requiring the constraint that $T/P_{\text{orb}} << 3/2\pi$ for the quadratic approximation to still be useful. Note that when the quadratic effect approaches minimum, the third order begins to dominate. Conversely, near the region of maximum quadratic effect, the third order is near minimum. Hence the most interference with quadratic recovery from the third-order term does arise near phase $\pi/4$. The restriction on practical integration times can be recast into a constraint on orbital periods searched. Fortunately, a large portion of parameter space is made accessible by quadratic transformations, extending useful integration times in binary pulsar searches by one to three orders of magnitude.

We now calculate the critical $\delta\alpha$ required to recover a broadening of the signal by precisely one channel for a period P_{crit}. Taking the derivative of the quadratic transformations (Eq. A2), we find

$$dt' = dt(1 + 2\delta\alpha t) \rightarrow \delta\alpha = (dt'/dt - 1)2t.$$

Evaluate for the total integration time T and require the transformation to stretch* the time series by the amount P_{crit}:

$$\delta\alpha = [(P_{\text{crit}} + T)/T - 1]/2T = P_{\text{crit}}/2T^2. \tag{A5}$$

*Incrementing the integration time by

$$\Delta T = P_{\text{Nyq}} \equiv 1 \text{ cycle at the Nyquist frequency}$$

adds one channel in the resulting Fourier power spectrum. Let $N_{ps} = T/2\tau_s$ = number of channels in power spectrum for integration time T, where τ_s is the sample interval. Then

$$T' = T + 2\tau_s = T + P_{\text{Nyq}}, \quad \text{and therefore } N_{ps}' = N_{ps} + 1.$$

Transformation ($T \rightarrow T'$) of a time series from one that contains a coherent signal to one where the signal begins at P_{Nyq}' and ends at P_{Nyq}' results in broadening by exactly one channel. The distribution of spectral power within the two channels depends on the specific transformation.

Coherence Recovery Realization In Time-Integrating Acousto-Optical Fourier Processors

In a time-integrating AO Fourier processor, two chirps of equivalent acceleration and duration modulate a coherent light source and are heterodyned to create a Fourier kernel. An additional phase with quadratic time dependence is manifested when the chirps have slightly different acceleration. The modified kernel can effect exact CR of a signal in a time series that has been quadratically time transformed; approximate recovery is realized for other functions. For signal $S(t)$, chirps C_1 and $C_1{}^*$ (complex conjugates), delay τ, chirp start frequency f_0, and chirp accelerations $\alpha \simeq \alpha'$,

$$S(v) = \int S(t)C_1(t,\tau)C_1{}^*(t,\tau)\,dt$$

$$= \int S(t)\exp j[(t+\tau)\{\alpha(t+\tau)+2\pi f_0\}]\exp j[-(t-\tau)\{\alpha'(t-\tau)+2\pi f_0\}]\,dt$$

$$= \int S(t)\exp j[4\pi f_0\tau + 2(\alpha+\alpha')t\tau + (\alpha-\alpha')(t^2+\tau^2)]\,dt. \tag{C6}$$

Letting $\alpha' = \alpha - \delta_\alpha$ and $\alpha'' = (\alpha' + \alpha)/2$ yields

$$S(v) = \int S(t)\exp j[\underset{(1)}{4\pi f_0\tau} + \underset{(2)}{4\alpha''t\tau} + \underset{(3)}{\delta\alpha(t^2+\tau^2)}]\,dt. \tag{C7}$$

The unequal chirps result in the terms labeled in Eq. (C7): (1) the usual acoustic fringe carrier (time-independent); (2) a Fourier kernel slightly modified from the equal chirp case, $4\alpha t\tau \rightarrow 4\alpha''t\tau$; and (3) an additional quadratic term in t. The τ^2 dependence in the third term represents an irrelevant, fixed spatial fringe pattern that, in practical realizations, is of vanishingly small magnitude compared to terms of interest. The t^2 phase in the integrand can remove a $-t^2$ phase in a signal. Let the signal

$$S(t) = \exp(j2\pi vt) \rightarrow S(t) = \exp j(2\pi vt + \gamma t^2). \tag{C8}$$

When $\delta_\alpha = -\gamma$, coherence is recovered exactly, and Eq. (C7) becomes

$$S(v) = \exp j[4\pi f_0\tau]\int S(t)\exp j[4\alpha''t\tau]\,dt, \tag{C9}$$

which is the usual time-integrating Fourier AO formulation, where the relationship between AOBD delay, τ, and frequency is $v = 2\alpha''\tau/\pi$. In many cases the quadratic transformation will be the best second-order approximation, and certainly the most straightforwardly generated analog implementation of CR, over a short interval to a more complex function, e.g., FM modulation arising from motion over a portion of an orbit or trajectory.

Appendix B

MARK II: FIGURES OF MERIT AND SPECIFICATIONS

Table B1 — Mark II Figures of Merit

Frequency resolution elements	$\sim 2^{15}$ (62500 pixels = present camera)/2
Input data rate	~350 MHz
Dynamic range	~500
Signal to noise	~25 (higher with increased light level)

Dynamic range increase (factor > 20) over two-dimensional time-integrating systems results from use of space integration in coarse frequency dimension; this provides the capability to detect very weak signals in the presence of strong, saturating signals.

Data rate increase over Mark I results from use of TeO_2 Bragg cells with center frequencies of 350 MHz to introduce signal and coarse reference chirp.

Space integration also enables gain of ~4 × over two-dimensional, purely time-integrating systems in useful input bandwidth of TeO_2 cell.

System throughput (bits/s), apart from postprocessing, is approximately two equivalent Cray-2s, by throughput comparison on FFT algorithm. The strictly acousto-optic portion of the system performs the transform ~500 times faster than Cray-2, but with less precision (see Table B2).

Table B2 — Throughput Comparison with State-of-the-Art Electronic Computer

Cray-2:	64-bit accuracy 10^6-point FFT in 1.24 s → (10^6/2-point spectrum) → 27 mbits/s throughput
AO Processor:	estimate ~4-bit accuracy (initially) ~10^6 points in ~2.5 ms with present camera and 2 pixels per frequency channel → 1/16 of spectrum recorded ~1 Gbits (= 4 bits × 0.35 GHz) input/16 = 67 Mbits/s throughput ~2 equivalent Crays (working speed)

*Accuracy increases with investment in improving light budget, postprocessing.

†AO processor does transform ~500 times faster than Cray-2.

Table B3 — Mark II Special Components

2 Specially engineered TeO_2 Acousto-optic Deflectors 200 MHz @ 3 dB, 5μs aperture Model 4350-1 Crystal Technology
1 Input Signal Driver for 4350-1 Deflector Model 1350-1 Crystal Technology
1 Fast chirp VCO 2.5-μs sweep, 0.5-μs dead-time phase-locked to 1°, < ±1 Hz @ each sweep start 100 MHz sweep uses center half of 4350-1 BW SO-350-200-XX Andersen Laboratories {Unit will be ~1.5 to 3 orders of magnitude faster than available digital sweeps}

Appendix C

VERIFICATION OF THE MARK II DESIGN BY USING THE SYMBOLIC MANIPULATION PROGRAM

We performed an automated verification of the Mark II acousto-optic design by using the Symbolic Manipulation Program (SMP). These computations served two purposes. First, it was necessary to verify that the processor would function according to specifications after modifying the original Bader [C1] design. Minor errors or misprints in Ref. C1 were uncovered in this process. These errors result in minor adjustments (phase shifts) to the mathematical representation and turn out to be irrelevant to the functioning of the processor. The corrected versions were verified by the SMP computations. Second, we were interested in exploring further modifications to the design, e.g., the realization of coherence recovery (CR) in a two-dimensional processor. SMP provides the capability of perturbing functions in a previously defined stream of calculations at any stage, thereby obviating manual reanalysis of the mathematical problem and simplifying evaluation of design changes.

An interpretation of the SMP input and output for the Mark II design follows. Equations that have one-to-one correspondence with "operations" are numbered. These are not necessarily in one-to-one correspondence with hardware elements since such elements may introduce more than one fundamental transformation. Other non-numbered equations are given for clarity.

The numbering system for the following equations divides them into four groups according to how they function in the calculation. Equations (S_i) are associated with inputs in the "signal" leg of the processor; Eqs. (C_i) characterize chirps introduced in the other ("reference") leg to analyze the input. Mathematical identities used to compute the output are not generally numbered. Finally, Eqs. (I_i) describe the results produced by the processor, corresponding to convolution integrals in the detector or output leg of the processor. (See Fig. 6 for the system overview showing the three legs.)

In one leg of an interferometer, the signal $S(t)$ is introduced by using an acousto-optic beam deflector (AOBD) of aperture D. $S(t)$ represents the amplitude of the acoustic information (i.e., the data—for simplicity, one unmodulated rf carrier within the Bragg cell [AOBD] bandwidth). The traveling acoustic wave is represented by $S(t - \xi/v)$, where ξ is the deflector coordinate (within the cell), approximately transverse to the light propagation vector, and v is the acoustic velocity. The diffracted light amplitude $A(x, t)$ is proportional to the acoustic signal amplitude.

Signal Input Leg:

The amplitude spectrum $U(f)$ of $S(t)$ is, by definition,

$$U(f) = \int dt\ S(t) \exp\{i 2\pi f t\}. .$$

(acoustic signal propagates through AOBD)

$$A(\xi,t) = S(t - \xi/v) \tag{S1}$$

(By Bragg diffraction, acoustic signal impressed onto light beam which passes through AOBD of aperture D; signal is now light amplitude)

$$A(\xi, t) = S(t - \xi/v) \text{ rect } (\xi/D),$$

where

$$\text{rect } (\xi/D) = 1 \quad \text{for } -D/2 \leq \xi \leq D/2$$

$$= 0 \quad \text{otherwise.} \tag{S2}$$

(light signal Fourier transformed by lens)

$$A(x, t) = \int d\xi\, S(t - \xi/v) \text{ rect } (\xi/D) \exp\{-2\pi\alpha x\xi\}, \tag{S3}$$

where x is the vertical (course frequency) detector coordinate, $\alpha = 1/(\lambda F)$, $\lambda =$ light wavelength, and $F =$ focal length of the Fourier transform lens. Equation S3 assumes that imaging from the signal AOBD's Fourier transform plane to the detector plane is one-to-one. $A(x, t)$ is in the detector plane, which is the imaged Fourier transform plane of the signal AOBD.

In the following, recognize the auxiliary variable $z = f/v$ (z is a scaled Fourier transform coordinate of the time t). Equation (S3) is reduced to another form, and an example of the convolution theorem is explicitly derived. First, let $t \rightarrow t - \xi/v$ (using shift theorem),

$$U(f) \exp\{i2\pi\xi/v\} = \int dt\, S(t - \xi/v) \exp\{i2\pi ft\},$$

and taking the Fourier transform of both sides,

$$\int \text{df } U(f) \exp\{-i2\pi f(t - \xi/v)\} = \int df\, U(f) \exp\{-i2\pi ft\} \exp\{i2\pi f\xi/v\} = S(t - \xi/v).$$

Substituting this result into Eq. (S3) gives

(Shift theorem used to transform time shift to phase shift)

$$A(x, t) = \int d\xi \int \text{df } U(f) \exp\{-i2\pi ft\} \exp\{i2\pi f\xi/v\} \text{ rect } (\xi/D) \exp\{-i2\pi\alpha x\xi\}. \tag{S4}$$

Now remembering that the FT of rect(x) is sinc$(\pi X) = \sin(\pi X)/\pi X$, df $= v \cdot dz$, and recognizing that a factor $1/v$ arises in the transformation $U(f) \rightarrow U(zv)/v$,

$$A(x, t) = \int v \cdot dz\, U(zv)/v \exp\{-i2\pi zvt\} \int d\xi \text{ rect } (\xi/D) \exp\{-i2\pi\xi(\alpha x - z)\},$$

(Integrate out ξ dependence)

$$A(x, t) = \int dz \exp\{-i2\pi zvt\}\, U(zv) \text{ sinc}[\pi D(\alpha x - z)]. \tag{S5}$$

Recapitulating, $A(x, t)$ is the diffracted light amplitude containing the information in the signal at the detector plane, having passed through the AOBD of width D and having been Fourier transformed by a lens. One effect of the latter is represented by the phase factor αx in the sinc function; also $U(zv)$ is the optical Fourier transform of the input signal.

Reference Leg:

In the other leg of the interferometer, a second AOBD, having properties identical to the signal AOBD, is driven by a periodic chirp of period T_1. The chirp has bandwidth Δf_1 and center frequency f_c, parameters that span the potential range of signal frequencies. This coarse chirp is represented by

(Acoustic chirp signal produced by chirp generator)

$$C_1(t) = \sum_n \text{rect}\,[(t - nT_1)/T_1]\,\exp\{i[a(t - nT_1)^2 + b(t - nT_1)]\}, \tag{C1}$$

where $a = \pi\Delta f_1/T_1$ and $b = 2\pi f_{\min}$, and a constant phase term ϕ_n in the b coefficient is suppressed for convenience (notice that the coarse chirp generator must supply chirps each beginning with this phase, $\phi_n = \phi_{\text{const}}$). This repeating chirp propagates through the AOBD and is Fourier transformed by a lens identical to the lens that transforms the signal beam. We proceed to determine the amplitude of the chirp light field in the detector plane:

(Chirp propagates through AOBD as acoustic signal)

$$C_1(t, \xi) = \sum_n \text{rect}\,[(t - nT_1 - \xi/v)/T_1]$$

$$\cdot\,\exp\{i[a(t - nT_1 - \xi/v)^2 + b(tnT_1 - \xi/v)]\}. \tag{C2}$$

(By Bragg diffraction, chirp impressed onto light beam that passes through AOBD of aperture D; chirp is now carried by light amplitude)

$$r(t, \xi) = \sum_n \text{rect}\,[(t - nT_1 - \xi/v)/T_1] \cdot \text{rect}\,(\xi/D)$$

$$\cdot\,\exp\{i[a(t - nT_1 - \xi/v)^2 + b(t - nT_1 - \xi v)]\}. \tag{C3}$$

(The optical Fourier transform of chirp is performed and imaged one-to-one to the detector plane)

$$R(t, x) = \int d\xi\, r(t, \xi)\,\exp\{-i2\pi\alpha\xi x\}$$

$$= \int d\xi\,\exp\{-i2\pi\alpha\xi x\} \sum_n \text{rect}\,[(t - nT_1 - \xi/v)/T_1] \cdot \text{rect}(\xi/D) \tag{C4}$$

$$\cdot\,\exp\{i[a(t - nT_1 - \xi/v)^2 + b(t - nT_1 - \xi/v)]\}.$$

In correspondence with the Convolution Theorem, make the associations

$$f = \sum \text{rect}[(t - nT_1 - \xi/v)/T_1] \exp\{i[a(t - nT_1 - \xi/v)^2 + b(t - nT_1 - \xi/v)]\}$$

and $g = \text{rect}(\xi/D)$, and the following result is straightforwardly obtained:

(Use Convolution Theorem to rearrange chirp)

$$R(t, x) = D \int dx' \, V(x - x', t) \, \text{sinc}[\pi\alpha D x'],$$

where

$$V(x, t) = \sum \int d\xi \exp\{i[a(t - nT_1 - \xi/v)^2 + b(t - nT_1 - \xi/v) - 2\pi\alpha\xi x]\}$$

$$\cdot \text{rect}[(t - nT_1 - \xi/v)/T_1]. \tag{C5}$$

In $V(x, t)$ make the substitution $z = t - nT_1 - \xi/v$, $-v dz = d\xi$ (note: rect function is symmetric and therefore introduces a minus sign, absorbing the minus that arises from $-v\,dz$):

(Variable change simplifies notation)

$$V(x, t) = v \sum_n \exp\{-2\pi\alpha v x(t - nT_1)\}$$

$$\cdot \int dz \exp\{iaz^2 + iz[2\pi\alpha v x + b]\} \text{rect}[z/T_1]. \tag{C6}$$

Again using the Convolution Theorem, transform the integral in Eq. (C6). The problem can be formulated such that the dual variables of the Fourier integral are z and $\alpha v x + b/2\pi$. In correspondence with the convolution theorem, make the associations

$$f = \text{rect}\{z/T_1\} \text{ and } g = \exp\{iaz^2\}.$$

The phase factor izb will appear in the transform of f as a shift and in the transform of g as a phase term.

To see how to arrive at Eq. (C7), first obtain the Fourier transform of g alone, then generate the convolution of the transforms of f and g. The trick is to use the transform property of a Gaussian.

Let $\alpha v x + b/2\pi = u$. Then,

$$\int dz \exp\{iaz^2\} \exp\{i2\pi uz\} = \int dz \exp\{-\pi [-iaz^2/\pi - 2iuz]\}.$$

Completing the square,

$$\int dz\ \exp\{-\pi\,[-iaz^2/\pi - 2iuz + (\pi/ia)u^2 - (\pi/ia)u^2]\} =$$

$$\exp\{-i(\pi u)^2/a\} \int dz\ \exp\{-\pi[z(-ia/\pi)^{1/2} - iu/(-ia/\pi)^{1/2}]^2\} =$$

Letting $z' = z(-ia/\pi)^{1/2} - iu/(-ia/\pi)^{1/2}$, $dz = (-ia/\pi)^{-1/2}dz'$, we get

$$\exp\{-i(\pi u)^2/a\} \int (i\pi/a)^{1/2}dz'\ \exp\{-\pi z'^2\} = (i\pi/a)^{1/2}\ \exp\{-i(\pi u)^2/a\}.$$

Now transform f and multiply with the folded transform of g, include the shifts arising from exp(*izb*, *substitute* $avx + b/2\pi$ for u, and arrive at a new expression for the *integral* in Eq. (C6):

(Identity to facilitate use of Convolution Theorem in Eq. (C6))

$$T_1\ K \int dx'\ \exp\{-i(\pi\alpha v)^2(x - x' + b/2\pi\alpha v)^2/a\} \cdot \mathrm{sinc}[\pi T_1(v\alpha x' + b/2\pi)], \qquad \text{(C7)}$$

where $K = (i\pi/a)^{1/2}$. Now proceed to simplify Eq. (C7) by an approximation, following Bader exactly. Expanding the exponent in Eq. (C7),

$$\exp\{-i(2\pi\alpha v)^2[x^2 + x'^2 + b^2/(2\pi\alpha v)^2 + xb/\pi\alpha v - 2xx' - x'b/\pi\alpha v]/4a\}$$

The $(x')^2$ term is negligible in the region over which the sinc function is significant: at one Rayleigh distance $x' = 1/(vT_1\alpha)$, and therefore

$$(\pi\alpha v x')^2/a = \pi/(\Delta f_1 T_1) = \pi/N_1 << 1,$$

where we have used the definition $a = \pi\Delta f_1/T_1$ and where N_1 is the number of resolvable frequencies in the coarse chirp. Moving the non-x' terms outside the $u = x + b/2\pi\alpha v$, Eq. C7 looks like

$$T_1\ K\ \exp\{-i\Psi\} \int dx'\ \exp\{i2\pi x'u[(2\pi\alpha v)^2/4\pi a]\}\ \mathrm{sinc}\pi T_1[v\alpha x' + b/2\pi].$$

Now letting

$$x'' = v\alpha x' + b/2\pi,\ x' = x''/v\alpha - b/2\pi v\alpha,\ \mathrm{dx}' = dx''/v\alpha, \text{ we get}$$

$$T_1\ K/v\alpha\ \exp\{-i\Psi\} \int dx''\ \exp\{i2\pi u(x''/v\alpha - b/2\pi v\alpha)(2\pi v\alpha)^2/4\pi a\}\ \mathrm{sinc}[\pi T_1 x'].$$

Now let

$$w = x''(2\pi\alpha v)^2/4\pi a v\alpha = x''\pi v\alpha/a,\ dx'' = (a/\pi v\alpha)dw:$$

$$T_1\ Ka/\pi(v\alpha)^2\ \exp\{-i\Psi\}\ \exp\{-i\pi b\alpha v u/a\} \int dw\ \exp\{i2\pi wu\}\ \mathrm{sinc}[\pi T_1 aw/\pi v\alpha].$$

Performing the Fourier integral and inserting $u = x + b/2\pi v\alpha$ results in

$$K/\pi v\alpha \exp\{-ib^2/2a\} \exp\{-i\Psi\} \exp\{-i\pi b\alpha vx/a\} \text{ rect } [\pi\alpha v(x + b/2\pi\alpha v)/T_1 a].$$

Let $c = (i\pi/a)^{1/2} \cdot [a/\pi\alpha] \exp\{-ib^2/2a\}$. Then we have from above substitutions and Eq. (C6),

$$V(x, t) = c \exp\{-i[2\pi\alpha vx + b]^2/4a\} \exp\{-i\pi b\alpha vx/a\} \text{ rect } [(\pi\alpha vx + b/2)/T_1 a]$$

$$\cdot \sum_n \exp\{-i2\pi\alpha vx(t - nT_1)\}.$$

Now, using $\Delta f_1 T_1 = N_1 = \alpha D^2$, $T_1 = D/v$, $a = \pi\Delta f_1/T_1$, and $b = 2\pi f_{\min}$, define the rect argument with respect to $f_{\min}$ (set $r = f_{\min}/\Delta f_1$; note that Bader defines $r = f_{\text{cen}}/\Delta f_1$; either way, the limits are consistent, see Eq. (C11)):

$$\text{rect } [\{\pi\alpha vx + b/2\}/T_1 a] = \text{rect } [\{\pi\alpha v^2 x/a + bv/2a\}/D].$$

Since $\pi\alpha v^2/a = \pi(\Delta f_1 T_1/D^2)(D^2/T_1^2)/(\pi\Delta f_1/T_1) = 1$, $bv/2a = Df_{\min}/\Delta f_{\min}/\Delta f_1 = rD$, then we have

(Several transformations to evaluate integral from Eq. (C6))

$$V(x, t) = c \exp\{-i[2\pi\alpha vx + b]^2/4a\} \exp\{-i\pi b\alpha vx/a\} \text{ rect } [(x + rD)/D] \tag{C8}$$

$$\cdot \sum_n \exp\{-i2\pi\alpha vx(t - nT_1)\},$$

where an extra phase ($\exp\{i\pi b\alpha vx/a\}$) is discovered that does not appear in Bader's derivation. The phase is physically meaningful: it represents the discontinuity from one coarse frequency line to the next and arises from a combination of the lens Fourier transform and the fast chirp. It is inconsequential, since we desire only the power and not the amplitude spectrum.

Continuing, use the identity $\sum_n \exp(ian) = 2\pi \sum_p \delta(a - 2\pi p)$,

where $\delta(x)$ is the Dirac delta function. Make the association $2\pi\alpha vxT_1 = a$ to arrive at

(Convert sum of exponentials to [approximate] sum of δs)

$$V(x, t) = c \exp\{-i[2\pi\alpha vx + b]^2/4a\} \exp\{-i\pi b\alpha vx/a\} \text{ rect } [(x + rD)/D]$$

$$\cdot \exp\{-i2\pi\alpha vxt\} \sum_p \delta(x - p/\alpha vT_1). \tag{C9}$$

In our modification, the slow chirp multiplies both legs (with opposite directions of propagation) by using AOBDs. The resulting deflections are in the y coordinate. The slow chirps propagating in the AOBDs with acceleration β (minus sign for signal leg, plus sign for reference leg) and start frequency f_0 are

$$C_2 = \exp\{i(t \pm \tau)(\beta(t \pm \tau) + 2\pi f_0)\}.$$

Detector Output Leg:

Applying the slow chirp to the signal leg (Eq. (S5)) yields the time-dependent signal contribution to the light amplitude at the detector:

(Signal amplitude multiplied by slow chirp)

$$A(x, t) = \exp\{i(t - \tau)[\beta(t - \tau) + 2\pi f_0]\} \int dz \exp\{-i2\pi zvt\}\, U(zv)\, \mathrm{sinc}[\pi D(\alpha x - z)]. \quad \text{(I1)}$$

Similarly, the slow chirp multiplying the coarse chirp reference (Eq. C11) yields

(Coarse chirp reference multiplied by slow chirp)

$$R(t, x) = C \sum_p \exp\{-i2\pi pt/T_1\}\, \mathrm{rect}\,[p/N_1 + r]\, \mathrm{sinc}[\pi T_1(\alpha vx - p/T_1)] \quad \text{(I2)}$$

$$\cdot \exp\{i(t + \tau)(\beta(t + \tau) + 2\pi f_0)\}.$$

The portion of the light bias offset arising from the signal leg of the interferometer is determined by taking the real part of the square of the light amplitude from Eq. (I1), integrating for the duration of the slow chirp T_2, and making the substitution $z = f/v$:

(Signal leg contribution to the light bias)

$$E_1 = T_2 \int \mathrm{df}\, \mathrm{sinc}[\pi D(\alpha x - f/v)]^2\, U(f). \quad \text{(I3)}$$

A similar calculation for the light bias arising from the coarse chirp leg yields

(Coarse chirp leg contribution to the light bias)

$$E_2 = C\, T_2\, \mathrm{sinc}[\pi(\alpha vxT_1 - p)]^2. \quad \text{(I4)}$$

Within constants (which are adjustable by varying the light levels in the two beams), Eqs. (I3) and (I4) represent the two light bias contributions: Equation (I3) defines the positive definite contribution on the line that contains the signal, with width determined by the finite AOBD aperture; Eq. (I4) defines the raster line pattern, with each reference line exhibiting a width resulting from Fourier transformation of the repeating coarse chirp (in Eq. (C9), summation of the exponentials produced the array of delta functions, or "comb" filter).